ELSEVIER

Journal of Chromatography A, 726 (1996) 211–222

JOURNAL OF CHROMATOGRAPHY A

Micellar electrokinetic capillary chromatography of high explosives utilising indirect fluorescence detection

Scott Kennedy[a,*], Brian Caddy[a], John M.F. Douse[b]

[a] *Forensic Science Unit, Strathclyde University, Royal College Building, 204 George Street, Glasgow G1 1XW, UK*
[b] *Defence Evaluation and Research Agency (DERA), Fort Halstead, Sevenoaks, Kent TN14 7BP, UK*

Received 25 July 1995; revised 12 September 1995; accepted 14 September 1995

Abstract

Indirect fluorescence detection was applied to the detection of the high explosives nitroguanidine (NGU), ethylene glycol dinitrate (EGDN), cyclotetramethylene tetranitramine (HMX), cyclotrimethylene trinitramine (RDX), nitroglycerine (NG), 2,4,6-trinitrotoluene (TNT), pentaerythol tetranitrate (PETN) and trinitrophenyl-methylnitramine (tetryl), separated by MEKC. Two fluorophores, fluorescein and rhodamine B, were investigated. All explosives except NGU and PETN were detected but sensitivity was poor. Some of this lack in sensitivity may be associated with laser instability.

Keywords: Micellar electrokinetic chromatography; Detectors, electrophoresis; Explosives

1. Introduction

Micellar electrokinetic chromatography (MEKC) was first reported by Terabe et al. in 1984 [1]. The application of this technique to the separation and identification of explosives was reported by Northrop and co-workers [2,3] and later applied to explosive contamination in soils by Kleiböhmer et al. [4].

Table 1
Explosives analysed

TNT	2,4,6-Trinitrotoluene
Tetryl (CE)	Trinitrophenyl-methylnitramine
NG	Nitroglycerine
PETN	Pentaerythol tetranitrate
RDX	Cyclotrimethylene trinitramine
HMX	Cyclotetramethylene tetranitramine
EGDN	Ethylene glycol dinitrate
NGU	Nitroguanidine

*Corresponding author.

Recent work conducted in these laboratories investigated the separation of the high explosives NGU, EGDN, HMX, RDX, NG, TNT and tetryl using UV detection [5]. In this report the detection of these explosives was attempted using indirect fluorescence detection (for abbreviations of the explosives analysed see Table 1).

Indirect fluorescence detection has recently been applied by Amankwa and Kuhr to neutral analytes separated by MEKC [6]. A fluorophore or visualisation agent was added to the buffer system which resulted in a constant, high-level background signal at the detector. The mechanism by which the analytes were detected was described by Takeuchi and Yeung [7] using reversed-phase liquid chromatography, in which the analytes perturb the partitioning of the visualisation agent between the mobile and stationary phases. In MEKC, the analytes perturb the partitioning of the fluorophore between the aqueous and micellar phases.

0021-9673/96/$15.00
SSDI 0021-9673(95)01013-0

One of the properties of micelles is their ability to alter the fluorescence quantum yields of a variety of fluorophores and thus boost the fluorescence signal. The micro-environment encountered by a molecule in a micellar system can be drastically different from that in bulk, homogeneous solvent systems. These differences have been explained in terms of the alteration of the solvent properties, e.g. local viscosity, polarity and the dielectric constant of a solute associated with the micelles [8]. The overall result is that the micelles protect the excited fluorophore from quenching/deactivation processes and promote de-excitation by radiative processes [9]. Thus, the fluorescence signal of a fluorophore associated with a micellar phase can be significantly enhanced over that of a free, bulk solution. Significant shifts in emission maxima in the presence of micelles have also been observed. [6].

The presence of a solute can either decrease the stability of the fluorophore–micelle complex or alter the distribution of fluorophore between the aqueous and micellar phases. This will result in a lowering of the fluorescence signal in the sample zone by displacement of the fluorophore and by alteration of the net fluorescence quantum yield of the fluorophore remaining within the sample zone. The fluorescence intensity recorded at the detector is the sum of the two fluorophore intensities, i.e. the fluorescence in the aqueous phase and the "enhanced" fluorescence in the micellar phase.

Detection of solutes which partition mainly in the aqueous phase will depend on the quenching of the fluorophore in the aqueous phase by the solute. This phenomenon may occur in the detection of explosive compounds since nitro groups are known to cause fluorescence quenching. When quenching of the fluorophore by a solute partitioned into the micellar phase was suspected, a considerably larger peak size was observed and at higher concentrations a non-linear relationship between peak height and concentration was noted by Amankwa and Kuhr [6]. When only displacement mechanisms were suspected a linear relationship across a wide concentration range was observed. Amankwa and Kuhr also observed that the peak-height integrals of micelle-solubilised solutes increased with fluorophore concentration until the fluorophore concentration matched the concentration of the micelles. Beyond the micelle concentration, the peak heights were found to level off while peak areas became broader. The detection of compounds that partition mainly into the aqueous phase can only be optimised when the fluorophore concentration is higher than the micelle concentration.

The sensitivity of this detection technique depends upon the stability of the fluorescence background. This is quantified as the dynamic reserve (DR) defined as the background signal divided by the signal noise (S/N 3:1). The limit of detection can be defined as C_{lim}, where:

$$C_{\mathrm{lim}} = C_{\mathrm{FLU}} \frac{1}{\mathrm{DR} \times \mathrm{TR}}$$

where C_{FLU} is the fluorophore concentration and TR is the transfer number, i.e. the number of fluorophore molecules displaced by the solute.

Unfortunately, unstabilised laser sources, as used in this investigation, tend to be noisy with low dynamic reserves of approximately 100 [10,11]. This may be compared with current-controlled light bulbs which can have dynamic reserves of up to 10 000 [11]. Laser noise can be controlled by using the double beam configuration [7,12] or more simply by feedback control of the laser light with commercially available laser-power stabilisers [13–15]. Although this results in a drop of laser power of approximately 40% [14], the dynamic reserves thus gained can be between 800 and 1000.

2. Experimental

2.1. Apparatus

Experiments were performed on a Beckmann P/ACE 2100 (Palo Alto, CA, USA) consisting of a 0–30 kV power supply, an autosampler, liquid cooling of the capillary and absorbance and fluorescence detectors. A deuterium lamp and a free-standing 3-mW argon-ion laser 488 nm (488 nm rejection, 520/20 nm bandpass) were available for each detection mode, respectively. This instrument allowed injection by two modes: pressure and electrokinetic. Data acquisition and analysis were conducted by computer, utilizing the Gold workstation software.

Fused-silica capillaries (polyimide-coated outside,

internally uncoated; 75 μm I.D., 373 μm O.D., 50 cm inlet to detector, 57 cm total length) were used for all experiments. These capillaries were supplied by Beckmann with preburned windows. The UV cartridge aperture was 100×200 μm. Prior to use, each day the capillaries were rinsed with acetone for 5 min, ethyl acetate and methanol for 2 min followed by 0.1 *M* NaOH and micellar buffer for 10 min each. Two-minute rinses of 0.1 *M* NaOH, water and micellar buffer were performed between analyses. The separation conditions were held constant at 19 μA. The temperature was maintained at 25°C. Injections were performed at low pressure (0.5 p.s.i., ca. 3.45 kPa) for 1 s.

2.2. Reagents

Sodium tetraborate buffer (20 mmol dm^{-3}, pH 8.5), pure water (Millipore-Q 0.22-μm filtered water was used in later work with no detectable difference) and 0.1 mol dm^{-3} NaOH were purchased from Fluka (Gillingham, Dorset, UK) and sodium dodecyl sulphate (SDS) was purchased from Aldrich (Gillingham, Dorset, UK). All explosive standards were supplied by the Forensic Explosives Laboratory, Defence Evaluation and Research Agency, Fort Halstead, Kent, UK.

The sodium tetraborate buffer was diluted 8-fold to produce a working concentration of 2.5 mmol dm^{-3}. The working micellar solution of 25 mmol dm^{-3} SDS was made freshly each day by the addition of the appropriate amount of SDS to the tetraborate solution with ultrasonication. Fluorophore (fluorescein) containing buffers were prepared by the addition of a concentrated aliquot of the fluorophore to the tetraborate solution each day. The micellar buffer was then filtered though a Whatman 0.45-μm polypropylene syringe filter (Laserchrom, Gravesend, Kent, UK) prior to use.

2.3. Procedure

Constrained by the solubility of the explosives, the stock solutions were prepared in ethanol at the following concentrations: HMX, 0.5 mmol dm^{-3}; RDX, 1 mmol dm^{-3}; PETN, 3 mmol dm^{-3}; NGU and tetryl (CE), 10 mmol dm^{-3}; TNT and NG, 50 mmol dm^{-3}; EGDN, 60 mmol dm^{-3}; and the internal standard 2-fluoro-5-nitrotoluene, 100 mmol dm^{-3}. All stock solutions were stored under refrigeration at 4°C until needed and were ultrasonicated and allowed to cool for 10–15 min prior to use each day.

Samples were prepared by diluting appropriate aliquots of the stock solutions in the SDS–tetraborate working buffer solution to a final volume of 5 ml, to produce solutions ranging from $1 \cdot 10^{-5}$ mol dm^{-3} to $1 \cdot 10^{-4}$ mol dm^{-3}. Due to the very low solubility of HMX and RDX in ethanol, the aliquots of these stock solutions necessary to produce a $1 \cdot 10^{-4}$ mol dm^{-3} explosive concentration in 5 ml total volume were unacceptably large. Therefore the aliquots for these two stock solutions were arbitrarily set at 250 μl, thus producing solutions of $2.532 \cdot 10^{-5}$ mol dm^{-3} and $5.178 \cdot 10^{-5}$ mol dm^{-3}, respectively, in an otherwise $1 \cdot 10^{-4}$ mol dm^{-3} solution. A 200-μl aliquot of the HMX and RDX stock solutions was used for $8 \cdot 10^{-5}$ mol dm^{-3} solutions and so on.

2.4. Reconstituted sample procedure

A clear micro-volume insert, 7×44 mm (Phase Separations, Clwyd, UK, Cat. No. 403800) was placed into a 4.5 cm^3, clear, glass vial (Phase Separation, Cat No. 404802). Aliquots of the stock solutions of the explosives, appropriate to produce $1 \cdot 10^{-4}$ mol dm^{-3} solutions (except for HMX and RDX) in a final volume of 250 μl, were syringed into the insert. The more volatile compounds were added last, in the order of NG, EGDN and finally 2-fluoro-5-nitrotoluene. The walls of the insert were then quickly washed with 50 μl of a 10% solution of the involatile keeper compound, glycerol, in ethanol. The sample was then gently blown down with nitrogen for 1–5 min until a minimum volume of approximately 5–10 μl was achieved. An amount of 250 μl of the micellar buffer solution was then added to the insert to produce a final sample solution containing approximately 2% v/v glycerol which was then ultrasonicated for 5 min. A volume of 25 μl of the sample was then transferred by a glass–metal syringe into the Beckmann microvial (5–30 μl working volume). The microvial was then placed upon a spring mounting and placed within a 4.5-ml vial. A volume of 0.5 ml of water was placed into

the bottom of each vial to maintain humidity and reduce sample evaporation.

3. Results and discussion

Indirect fluorescence detection of explosives in MEKC using fluorescein dye as the visualisation agent was explored. Fluorescein absorbs well at 488 nm and has a fluorescence spectrum that produces a strong signal in the 510–530 nm region exhibiting a maximum at approximately 520 nm. Fluorescein was chosen by Beckmann for the calibration of the fluorescence detector by virtue of its strong signal in this wavelength region. As mentioned earlier, micellar phases have been found to cause shifts in emission spectra maxima [6]. Therefore tetraborate buffer solutions containing fluorescein at a concentration of $1 \cdot 10^{-4}$ mol dm^{-3} with and without SDS (25 mmol dm^{-3}) were observed under a long-wave UV lamp to observe their fluorescent colour. When these solutions were passed through the capillary column under high pressure or were driven under a 19-μA current, the detector became overloaded (1000 relative fluorescence units, RFU, maximum). Thus, several fluorescein solutions of different concentrations were tested to find the concentration acceptable for fluorescein quenching measurements. A fluorescein concentration of $1 \cdot 10^{-5}$ mol dm^{-3} also overloaded the detector, but a $1 \cdot 10^{-6}$ mol dm^{-3} fluorescein solution produced signals of 119.76 and 118.48 RFU with and without SDS, respectively, and 111.15 RFU for an SDS-containing solution electrically driven at 19 μA. A fluorescein concentration of $1 \cdot 10^{-8}$ mol dm^{-3} produced signals of 1.45, 1.95 and 1.64 RFU when tested in the same way. It can be seen that solutions containing SDS do produce a slight, but relatively small, increase in fluorescence signal. The constant-current separations of the micellar fluorescein solutions can be seen to produce fluorescence signals with a size similar to those observed under high-pressure rinse.

Investigative work conducted using a $1 \cdot 10^{-6}$ mol dm^{-3} fluorescein concentration quickly encountered several problems with the electropherograms produced. A typical blank electropherogram obtained without injection gave a noisy baseline/background signal which was prone to disturbances. Large baseline disturbances were generated using a standard 1-s injection of a solution containing the same proportions of ethanol and micelle solution as would be used in a standard $1 \cdot 10^{-4}$ mol dm^{-3} explosive sample. A micelle solution containing approximately 20% (v/v) ethanol, i.e. 1 ml of ethanol diluted into a 5-ml total volume of micellar solution, produced the trace illustrated in Fig. 1. This baseline disturbance was attenuated on increasing the injection time to 5 s as seen in Fig. 2. These observations are most probably due to disturbances in the distribution of fluorescein within the buffer solution as a whole, aqueous and micellar phases, resulting in zones of relatively higher and lower concentrations. Mechanistic interpretations of the processes involved in the production of similar peaks have been proposed by Stranahan and Deming and in this case may be associated with changes in polarity and density caused by the presence of ethanol [16]. Similarly, 1-s injections of blank solutions containing the alternative solvents acetone and ethyl acetate produced electropherograms similar to those shown in Figs. 1,2.

The large positive peak observed at approximately 3.1 to 3.2 min is known as the system peak and is generated by the fluorophore being displaced from the micellar phase into the aqueous phase in the original injected sample zone. Due to a net drop in net quantum yield this initially results in a drop in fluorescence signal. Under electrophoretic separation, the aqueous zone migrates under electroosmotic flow while analytes are slowed and separated according to the degree of micellar-phase solubilisation exhibited. As a result, a separation between analytes and the displaced fluorophore in the aqueous phase occurs over time. Where the fluorophore concentration is not sufficient to completely complex all the micelles in the buffer, the additional fluorophore in the aqueous phase will be repartitioned into the uncomplexed micelles as the aqueous zone migrates towards the detector. If recomplexing is not completed before the zone reaches the detector, the local increase in fluorophore concentration due to excess in the aqueous phase, results in a positive signal [6,16]. Although fluorescein bears a negative charge at pH 8.5, electromigration is believed to be minor in comparison to the electroosmotic flow at this solution pH [17]. However, any negative electrophoretic migra-

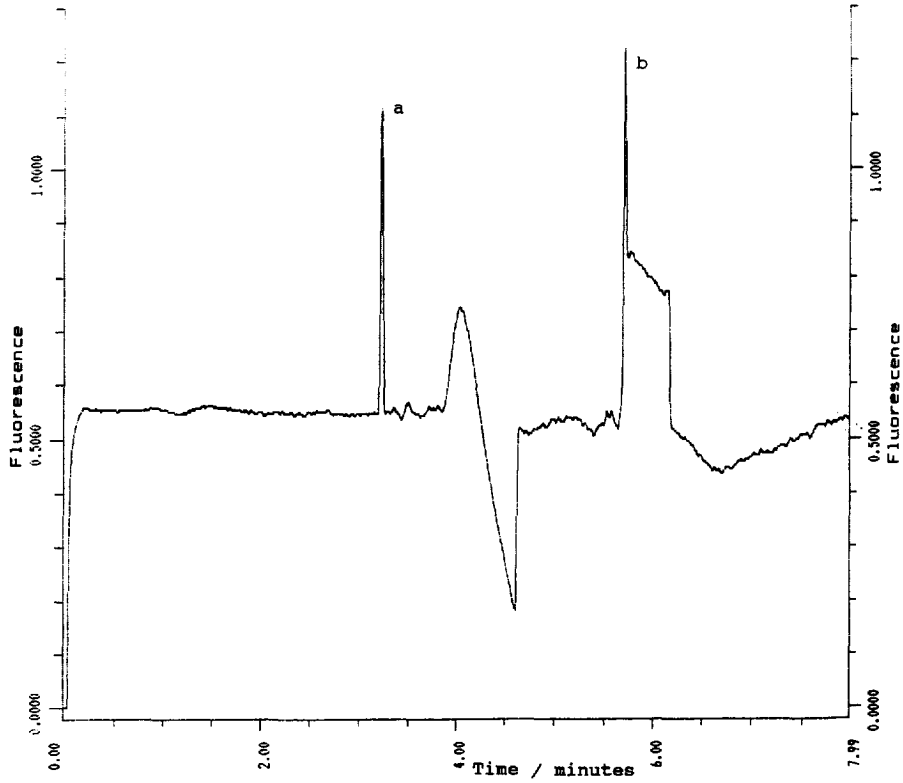

Fig. 1. Baseline disturbances caused by a 1-s injection and analysis of a ethanol–micelle (1:5, v/v) solution. Constant-current separation of 19 μA. Column temperature, 25°C. Buffer, 2.5 mmol dm^{-3} sodium tetraborate pH 8.5, 25 mmol dm^{-3} sodium dodecyl sulphate. Fluorescein concentration, $1 \cdot 10^{-6}$ mol dm^{-3}. Fluorescence detection, 488 nm excitation, 520/20 nm bandpass. Peak identity: (a) system peak; (b) unknown.

tion the fluorescein may undergo may shift it into a position to interfere with the detection of the NGU peak which is known to elute just after the electroosmotic flow itself [5]. A secondary mechanism, which may explain the depletion gradient observed in Fig. 2, may also be in operation. Ethanol and acetone have been noted to cause disruption of micelle formation by increasing the critical micelle concentration (CMC) [18,19]. Under electrophoretic conditions, the micelle-solubilised fluorophore will migrate slower than the electroosmotic flow. As a result, some fluorophore-complexed micelles will probably enter the solvent solution zone from the zone preceeding the sample. On encountering the solvent zone, the micelles may collapse into unassociated molecules and in the process "dump" their fluorophore load into the aqueous phase. This process would most probably result in an area of high fluorophore concentration followed by a fluorophore-poor zone as seen in Fig. 2. The later section of the electropherogram, i.e. corresponding to approximately 5 min and thereafter, may indicate the leading edge of replenished solution entering from the inlet buffer vial.

Both the system peak and the baseline distortions can be seen in the separation of a standard explosive sample as illustrated in Fig. 3. The large peaks for TNT, tetryl and the internal standard 2-fluoro-5-nitrotoluene can be clearly identified. These compounds are solubilised to a large degree by the micelles and cause a significant disruption of fluorophore distribution between aqueous and micellar phases. Quenching of the fluorophore by these compounds is also suspected. Hence the large peaks observed. The smaller negative peak observed after the system peak corresponds to the explosive EGDN.

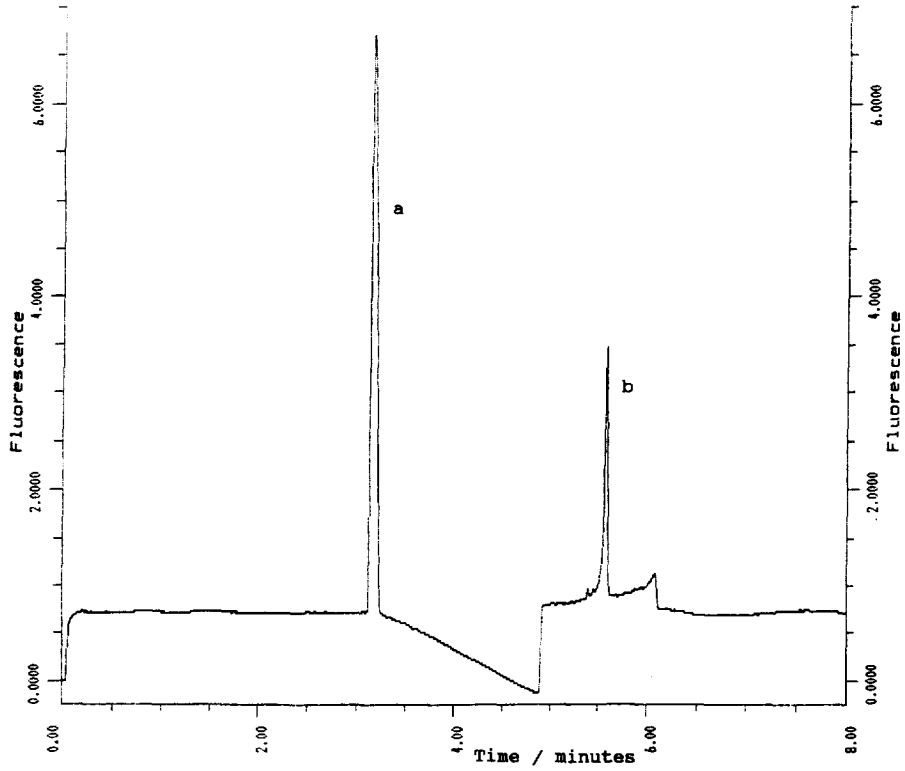

Fig. 2. Baseline disturbances caused by a 5-s injection and analysis of a ethanol–micelle (1:5, v/v) solution. All other conditions as in Fig. 1. Peak identity: (a) system peak; (b) unknown.

The peaks for NGU, HMX, RDX and PETN are not seen in this electropherogram which is obtained at a lower sensitivity than the analysis of a similar sample using UV detection at 214 nm [5] (Fig. 4). The elution position of NGU indicates a minimal interaction with the micellar phase. Therefore this explosive will exert little effect on the distribution of the fluorophore between the aqueous and micellar phases. The generation of a negative peak for this explosive thus depends mainly upon the displacement or quenching of fluorophore that may be present within the aqueous phase. A peak which in the case of NGU may be obscured by the large positive system peak. Due to their higher degree of micelle solubilisation, the generation of peaks for HMX and RDX will depend less upon interaction with aqueous fluorophore than for NGU. However, as mentioned earlier, both are present in this sample at relatively lower concentrations than the other explosives. Observation of the PETN peak could be obscured by the TNT and tetryl peaks which elute to either side [5]. Additionally, explosives which produce small peaks could be obscured by baseline noise. The system peak and the positive/negative baseline disturbances occurring next to the strong TNT and tetryl peaks can be reduced but are not eliminated when the samples are blown down to a small volume and reconstituted in micellar phase prior to injection. This can be observed in Fig. 5. Unfortunately, since the blowing down process discriminates against the more volatile components, the EGDN peak is absent. Amankwa and Kuhr [6] reported that peak integrals were maximised as the fluorophore concentration approached the point of saturation of the micellar phase. The micelle concentration (MC) can be calculated from the follow-

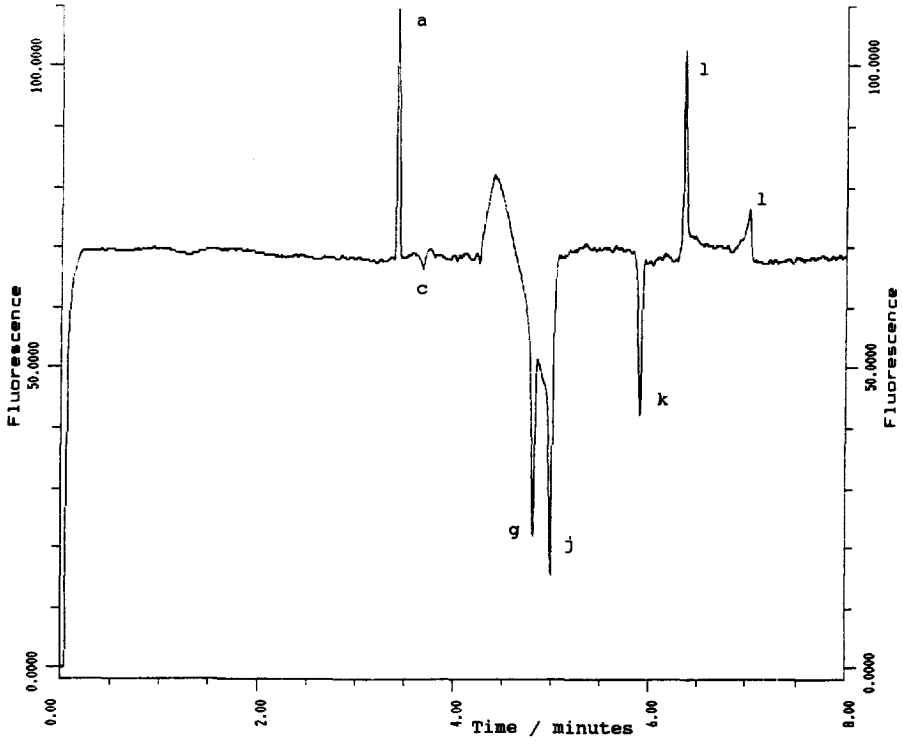

Fig. 3. Multi-component explosive sample analysed in a buffer containing $1 \cdot 10^{-6}$ mol dm^{-3} fluorescein. All other conditions as in Fig. 1. Peak identity: (a) system peak; (c) EGDN; (g) TNT; (j) tetryl; (k) 2-fluoro-5-nitrotoluene; (l) unknown.

ing expression:

$$MC = \frac{\text{SDS concentration} - \text{CMC}}{\text{SDS aggregation number}}$$

$$MC = \frac{(25 - 8.1) \cdot 10^{-3}}{62}$$

$$MC = 2.73 \cdot 10^{-4} \text{ mol dm}^{-3}$$

From high-pressure rinsing tests, it was found that a $6 \cdot 10^{-6}$ mol dm^{-3} fluorescein concentration was the upper limit of the detector for this particular system. This concentration of fluorescein produced RFU values of 979.74 and 914.41 under high-pressure rinsing and 19-μA separation, respectively (1000 RFU detector maximum). These values should be compared to RFU values of 119.76 and 111.15 obtained under similar testing for a $1 \cdot 10^{-6}$ mol dm^{-3} fluorescein concentration.

It can be seen that fluorescein produces too large a fluorescence signal for its concentration to be optimised to match the micelle concentration and thus produce the largest peak integrals. The optimisation of the peak integrals of components which partition mainly into the aqueous phase, i.e. NGU and EGDN, depends greatly on the fluorophore concentration in the aqueous phase. This optimisation will only occur when a substantial proportion of the fluorophore also resides in the aqueous phase, a situation that will only arise when the micellar phase is saturated. This cannot be achieved with fluorescein since the highest concentration of this fluorophore which can be supported by the detector is almost a factor of 100 below the micelle concentration. The increase in fluorophore concentration from 1 to $6 \cdot 10^{-6}$ mol dm^{-3} does result in an increase in explosive signal size but also results in an increase in the baseline noise as shown in Fig. 5. This is reflected in

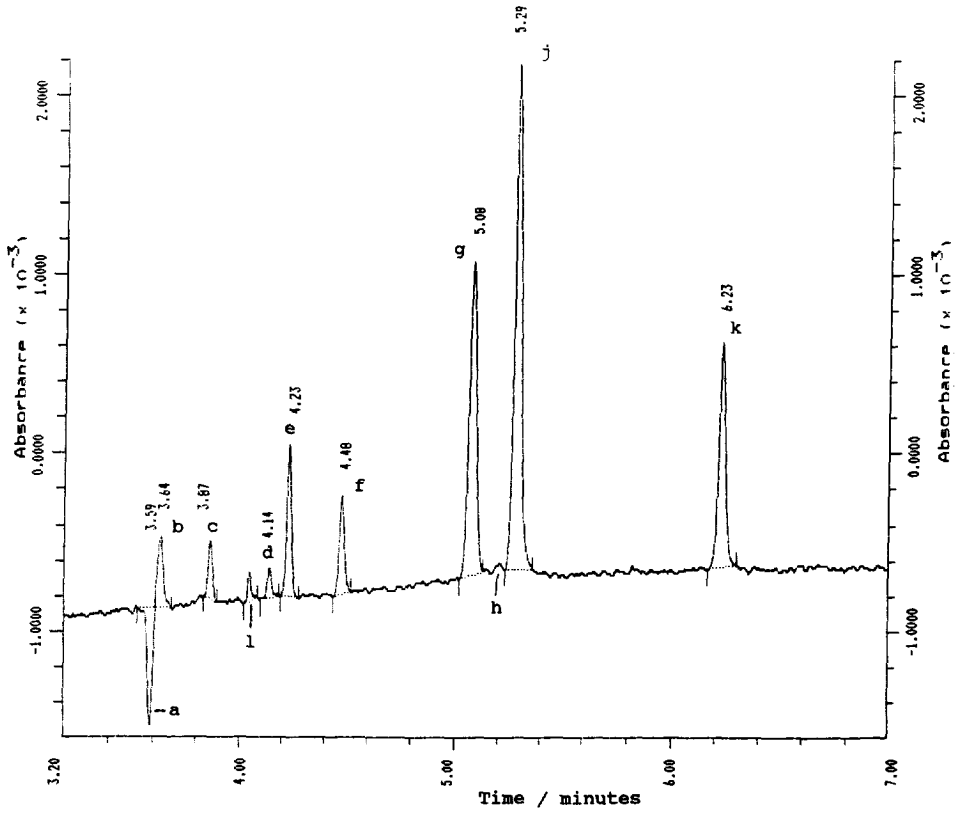

Fig. 4. Multi-component explosive sample separated under a constant current of 19 μA. Sample component concentration of $1 \cdot 10^{-4}$ mol dm^{-3}. Column temperature, 25°C. Buffer, 2.5 mmol dm^{-3} sodium tetraborate, 25 mmol dm^{-3} sodium dodecyl sulphate. One-second injection. UV detection at 214 nm. Peak identity: (a) ethanol; (b) NGU; (c) EGDN; (d) HMX; (e) RDX; (f) NG; (g) TNT; (h) PETN; (j) tetryl; (k) 2-fluoro-5-nitrotoluene; (l) unknown.

the calculations of dynamic reserve, a measure of sensitivity in an indirect detection system. This was seen to drop as fluorescein concentration increased (Table 2).

3.1. Calculations of dynamic reserve

A section of the baseline noise was integrated. The largest peak height was taken and multiplied by a factor of 3 to correspond to a signal-to-noise ratio of 3:1. The dynamic reserve was then calculated by dividing the background signal (obtained in the first 1/2 min of analysis prior to autozero) by the calculated noise level.

The baseline noise increased faster than the background signal resulting in a drop in dynamic reserve. It has been noted by Garner and Yeung [15] that the baseline of a fluorescein fluorescence signal becomes erratic when the buffer system pH was increased above pH 7. Unfortunately, when the pH of the buffer was reduced from pH 8.5 to pH 7.6 the resolution of the electropherogram was lost with an unstable baseline dropping in intensity and the production of low broad peaks eluting at the later times of 10–15 min. This was most probably due to the suppression of the electroosmotic flow at the lower buffer pH.

A peak was observed for RDX when its true concentration was increased to $1 \cdot 10^{-4}$ mol dm^{-3}. Similarly, NG was observed when the concentration was increased to $4 \cdot 10^{-4}$ mol dm^{-3}. The true HMX

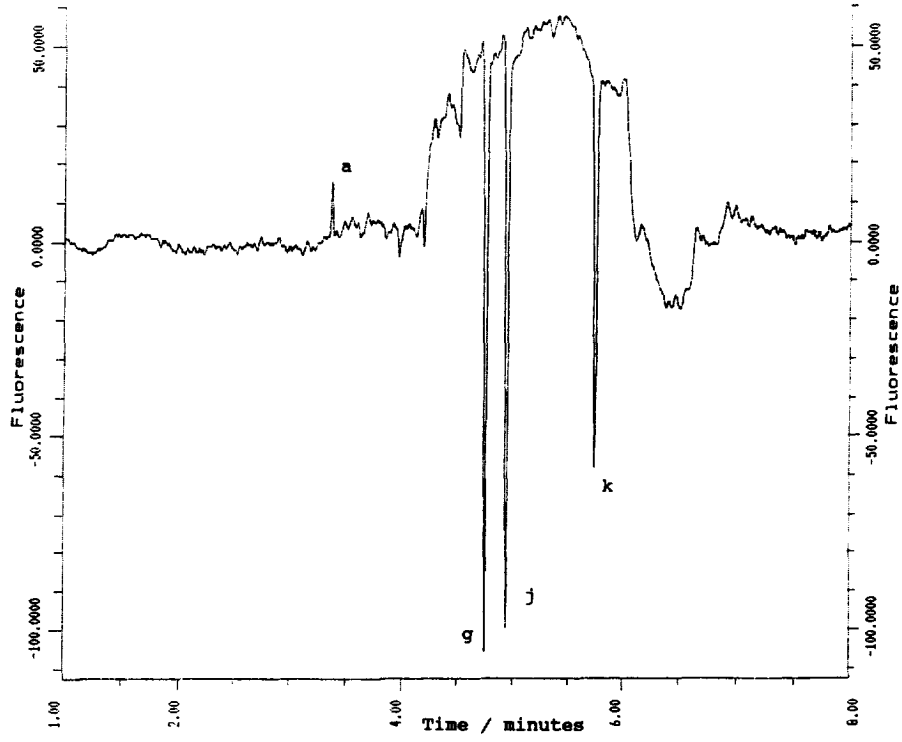

Fig. 5. Multi-component explosive sample analysed after being blown down and reconstituted in micellar phase. Fluorescein concentration in the buffer was $6 \cdot 10^{-6}$ mol dm^{-3}. All other conditions as in Fig. 1. Peak identity: (a) system peak; (g) TNT; (j) tetryl; (k) 2-fluoro-5-nitrotoluene.

Table 2
Calculated dynamic reserves for various fluorescein concentrations

Fluorescein (mol dm^{-3})	DR (peak height S/N=3:1)
$1 \cdot 10^{-6}$	71.97
$3 \cdot 10^{-6}$	55.47
$5 \cdot 10^{-6}$	41.43
$6 \cdot 10^{-6}$	36.84

concentration was increased to $8 \cdot 10^{-4}$ mol dm^{-3} without detection. NGU was not detected.

The positions of EGDN, RDX, TNT, NG, tetryl and 2-fluoro-5-nitrotoluene were confirmed by spiking.

Overall, the system is relatively insensitive with very poor dynamic reserve values. Sensitivity improvements can only be achieved using laser stabilisation and a different choice of fluorophore where concentration can be optimised to suit the micellar phase.

Other organic compounds, anthracene, eosin and rhodamine B, which are known to give similar fluorescent effects to fluorescein were tested for possible future application in an indirect detection

Table 3
Long-wavelength UV appearance of fluorophores with and without the addition of SDS

Compound	Long-wavelength UV appearance		Comments
	No SDS	SDS	
Eosin	Green–yellow	Green–yellow	No observable difference
Rhodamine B	Dull red	Bright orange	Shift towards blue on addition of SDS
Anthracence	Sky blue	Sky blue	No observable difference

scheme. Each compound was made up in solution to a concentration of $1 \cdot 10^{-4}$ mol dm^{-3} with and without 25 mmol dm^{-3} SDS (note that anthracene has a low solubility in water of $2.2 \cdot 10^{-7}$ mol dm^{-3}. Therefore saturated solutions were prepared in tetraborate buffer instead.) The results are presented in Table 3.

These solutions were rinsed under high pressure through the capillary and the corresponding RFU signals noted. Anthracene and eosin were found to be unsuitable, the former producing no detectable fluorescence signal, the latter giving a decrease in signal on addition of SDS, i.e. the opposite of what is desired. Moreover, a signal strength of 447.01 RFU detected for a $1 \cdot 10^{-4}$ mol dm^{-3} eosin concentration suggests that it is unlikely that the eosin concentration could be increased to much more than $2 \cdot 10^{-4}$ mol dm^{-3} without overloading the detector. Therefore optimisation of the fluorophore concentration to saturate the micellar phase would not be possible. Rhodamine B was found to be more suitable, producing RFU signals of 4.80 and 5.31 for non-SDS and SDS-containing solutions, respectively. These signals increased on the addition of SDS but remained low enough to allow optimisation of the fluorophore concentration so that it matched that of the micellar phase. Some preliminary investigations were therefore carried out using rhodamine B as the visualisation agent. Several similarities to the results obtained for fluorescein-containing solutions were obtained. High-pressure rinse testing of tetraborate solutions containing 1, 2 and $3 \cdot 10^{-4}$ mol dm^{-3} rhodamine B with and without SDS were conducted. The corresponding RFU signals observed under 19-μA constant-current separation of the SDS-containing solutions were also recorded. The RFU signals observed for $1 \cdot 10^{-4}$ mol dm^{-3} rhodamine B solution were 24.706, 24.883 and 23.765 for pressure-rinsed non-SDS, SDS and current-driven SDS solutions, respectively. For a rhodamine B solution of concentration $2 \cdot 10^{-4}$ mol dm^{-3}, corresponding RFU of 38.398, 43.720 and 41.715 were obtained which changed when using a solution of $3 \cdot 10^{-4}$ mol dm^{-3} to 46.647, 43.318 and 41.852. It can be seen that an increase in signal size with the addition of SDS for the 1 and $2 \cdot 10^{-4}$ mol dm^{-3} solution occurs. At a concentration of $3 \cdot 10^{-4}$ mol dm^{-3} minor changes occur and the signal of the SDS-containing solution under constant-current separation appears to have reached a maximum. Constant-current separation of the rhodamine B–SDS tetraborate solution produces baselines which have a sudden, sharp, step increase at approximately 5 min with the baseline, thereafter becoming steady on a new level, approximately 3 to 4 RFU higher. A similar baseline jump was observed with the higher fluorescein concentrations (Fig. 5), but this phenomenon occurs slightly later in the electropherogram with rhodamine B. A 1-s injection of a blank ethanol–micelle solution also produces baseline distortions similar to those observed with fluorescein (Fig. 1). Injections of a blown down and reconstituted multi-component explosive sample produces electropherograms such as Fig. 6. The peaks for TNT and tetryl can be clearly seen as before when using fluorescein. The identity of the 2-fluoro-5-nitrotoluene peak could not be confirmed, possibly through evaporative loss during blowing down of the sample. The peak for RDX can be seen without the increase in concentration necessary for fluorescein solutions. The slightly later time at which the baseline jumps in signal size allows detection of the NG peak without spiking. The peak sizes can also be seen to increase in size as rhodamine B concentration is increased. NGU was not detected in this preliminary work.

The dynamic reserve values calculated for these solutions are approximately twice those obtained for the fluorescein solutions as can be seen from Table 4.

Although not confirmed, this indicates that an optimum dynamic reserve may also exist alongside an optimal concentration of fluorophore to generate the background signal.

Overall, the use of rhodamine B as a fluorophore results in a more stable baseline and greater sensitivity than found with fluorescein. Further investigation into this matter is required.

4. Conclusions

Indirect fluorescence detection using fluorescein as the fluorophore permitted the detection of EGDN, RDX, NG, TNT, tetryl and 2-fluoro-5-nitrotoluene, the later-eluting compounds producing the stronger peaks. Due to baseline noise the sensitivity is lower

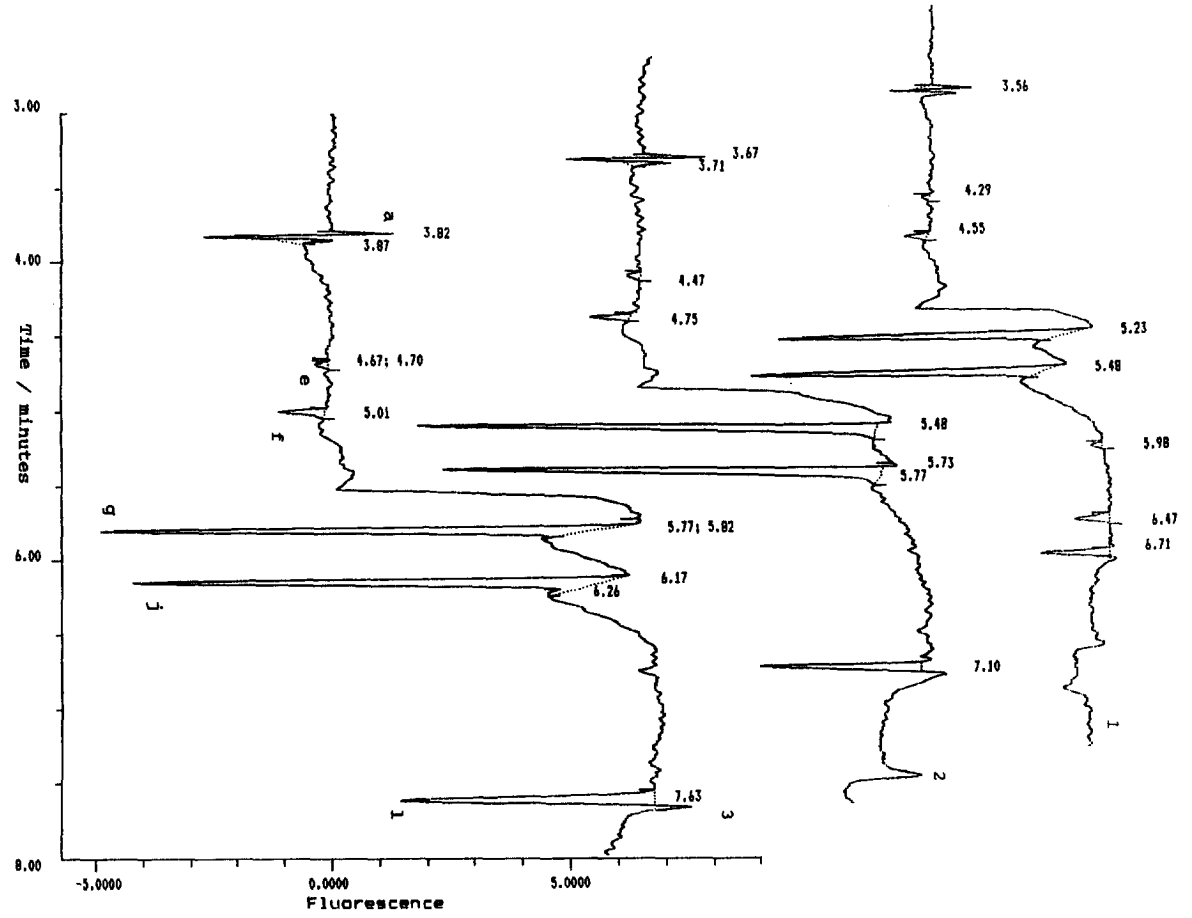

Fig. 6. Multi-component explosive sample analysed after being blown down and reconstituted in micellar phase. Rhodamine B concentration in chromatogram: (1) $1 \cdot 10^{-4}$ mol dm^{-3}; (2) $2 \cdot 10^{-4}$ mol dm^{-3}; (3) $3 \cdot 10^{-4}$ mol dm^{-3}. All other conditions as in Fig. 1. Peak identity: (a) system peak; (e) RDX; (f) NG; (g) TNT; (j) tetryl; (l) unknown.

than that found with UV detection. HMX was detected on an 8-fold increase in concentration and NGU remained undetected. Better sensitivity may be achieved with a different fluorophore which allows optimisation of its concentration to match the micelle concentration and with laser-power stabilisation.

Preliminary investigations on the use of rhodamine B as a fluorophore showed improved sensitivity and detection of RDX and NG without spiking.

Table 4
Calculated dynamic reserves for various rhodamine B concentrations

Rhodamine B (mol dm^{-3})	DR (peak height S/N=3:1)
$1 \cdot 10^{-4}$	120.384
$2 \cdot 10^{-4}$	132.830
$3 \cdot 10^{-4}$	106.176

Acknowledgments

This work was performed on instrumentation and with funding provided by the Forensic Explosives Laboratory, Defence Evaluation and Research Agency, Fort Halstead, Kent, UK and by the EPSRC. The study has been carried out with the support of Drs. M. Marshall, R. Hiley, S. Wanogho, Mrs. S.J. Letherby and fellow staff at The Forensic Explosives laboratory, The Defence Evaluation and Research Agency, Fort Halstead, Kent. We would also like to

thank Drs. M. Cole, J. Thorpe, E. McKenzie, A. Bennett, Mr. F. Drum, Ms. P. Flanagan and Mrs. B. Ottaway of Strathclyde University for their support and guidance. Thanks are also expressed to the staff of Beckmann Instruments, UK.

References

[1] S. Terabe, K. Otsuka, K. Ichikawa, A. Tsuchiya and T. Ando, Anal. Chem., 56 (1984) 111.
[2] D.M. Northrop, D.E. Martire and W.A. MacCrehan, Anal. Chem., 63 (1991) 1038.
[3] D.M. Northrop and W.A. MacCrehan, J. Liq. Chromatogr., 15 (1992) 1041.
[4] W. Kleiböhmer, K. Cammann, J. Robert and E. Mussenbrock, J. Chromatogr., 638 (1993) 349.
[5] Unpublished results
[6] L.N. Amankwa and W.G. Kuhr, Anal. Chem., 63 (1991) 1733.
[7] T. Takeuchi and E.S. Yeung, J. Chromatogr., 366 (1986) 145.
[8] H.N. Singh and W.L. Hinze, Analyst, 107 (1982) 1073.
[9] W.L. Hinze, H.N. Singh, Y. Baba and N.G. Harvey, Trends Anal. Chem., 3 (1984) 193.
[10] W.G. Kuhr and E.S. Yeung, Anal. Chem., 60 (1988) 1832.
[11] E.S. Yeung and W.G. Kuhr, Anal. Chem., 63 (1991) 275A.
[12] S.-I. Mho and E.S. Yeung, Anal. Chem., 57 (1985) 2253.
[13] W.G. Kuhr and E.S. Yeung, Anal. Chem., 60 (1988) 2642.
[14] L. Gross and E.S. Yeung, Anal. Chem., 62 (1990) 427.
[15] T.W. Garner and E.S. Yeung, J. Chromatogr., 515 (1990) 639.
[16] J.J. Stranahan and S.N. Deming, Anal. Chem., 54 (1982) 1540.
[17] J.W. Jorgenson, K. De Arman Lukacs, Anal. Chem., 53 (1981) 1298.
[18] D.W. Armstrong, Sep. Purif. Methods, 14 (1985) 213.
[19] P. Mukerjee and A. Ray, J. Phys. Chem., 67 (1962) 190.